Experimental Study on Flame Structure and Temperature Characteristics in a Lean Premixed Model Gas Turbine Combustor

Jong Ho Lee, Chung Hwan Jeon*, Young June Chang
School of Mechanical Engineering, Pusan National University,
San 30, Jangjeon-dong, Geumjeong-gu, Pusan 609-735, Korea
Chul Woong Park
Laser metrology group, Korea Research Institute of Standards and Science,
Daejon 305-600, Korea
Jae Won Hahn
School of Mechanical Engineering, Yonsei University,
Seoul 120-749, South Korea

Experimental study was carried out in an atmospheric pressure, laboratory-scale dump combustor showing features of combustion instabilities. Flame structure and heat release rates were obtained from OH emission spectroscopy. Qualitative comparisons were made between line-integrated OH chemiluminescence image and Abel-transformed one. Local Rayleigh index distributions were also examined. Mean temperature, normalized standard deviation and temperature fluctuations were measured by coherent anti-Stokes Raman spectroscopy (CARS). To see the periodic behavior of oscillating flames, phase-resolved measurements were performed with respect to the pressure wave in the combustor. Results on system damping and driving characteristics were provided as a function of equivalence ratio. It also could be observed that phase resolved temperatures have been changed in a well-defined manner, while its difference between maximum and minimum reached up to 280K. These results would be expected to play an important role in better understanding of driving mechanisms and thermo-acoustic interactions.

Key Words : Combustion Instability, Phase-resolved Gas Temperature, Coherent Anti-stokes Raman Spectroscopy (CARS)

Nomenclature

Alphabetic

a : Sound velocity [m/s]
f : The frequency of the pressure wave [Hz]
l : The length of the combustor [m]
p' : Pressure fluctuation
q' : Heat release fluctuation
R : Gas constant [kJ/kg-K]
T : Mean temperature in the combustor [K]

Greeks

α : Time delay between the trigger and flash-lamp [μs]
β : Time delay between flashlamp and Q-switch [μs]
ϕ : equivalence ratio
θ : The phase of pressure [deg.]
τ : The period of combustion instability [ms]

* Corresponding Author,
E-mail : chjeon@pusan.ac.kr
TEL : +82-51-510-3051; **FAX** : +82-51-512-5236
School of Mechanical Engineering, Pusan National University, San 30, Jangjeon-dong, Geumjeong-gu, Pusan 609-735, Korea. (Manuscript **Received** December 9, 2004; **Revised** April 15, 2005)

1. Introduction

Gas turbine combustion has been widely utilized to provide both ground-based power gener-

ation and propulsion for aero applications. It is accentuated by the fact that increased combustion temperature and high pressure ratio improve the thermal engine efficiency. Recently, owing to the increasingly stringent NOx emission regulations, most of motivations for understanding the dynamic and coupled phenomena associated with gas turbine combustions are mainly driven by a need to reduce the amount of pollutants produced while improving the efficiency of combustion devices (McDonell and Samuelsen, 2000). Among the low-emission technologies developed or suggested so far, lean premixed pre-vaporized combustion has been considered as an effective means to meet current and future NOx emission regulations while also providing acceptable performances (Docquier and Candel, 2002; Lefebvre, 1999; Seo, 2003). In case of lean premixed combustion, gas turbine combustors have to be operated in a narrow range of equivalence ratio near to the lean blow-out limit to obtain low NOx and CO emission levels simultaneously. Unfortunately, the lean premixed combustors are known to be susceptible to combustion instabilities. And many efforts have been devoted to suppress or avoid these combustion instabilities which are frequently linked to thermo-acoustic phenomena. Combustion instabilities are affected by many mechanisms such as combustor geometry, local heat release rates, vortex shedding and perturbation of equivalence ratio. Many works have been carried out to identify the mechanisms of driving instabilities (Lee et al., 2000; Venkataraman et al., 1999). Details on each mechanism and its active control schemes have been described in the excellent review articles (McManus et al., 1993; Zinn and Neumeier, 1997).

In characterizing unstable combustion in lean premixed combustors, though some caution should be used in applying emission spectroscopy for flame diagnostics, naturally occurring flame chemiluminescence such as OH^*, CH^* and CO_2^* has proven very useful. Extensive studies have been conducted to investigate the relationship between the rate of heat release and chemiluminescence emission (Samaniego et al., 1995; Dandy and Vosen, 1992; Najm et al., 1998), which have shown that the location of the chemiluminescence emission could be used as an indicator of the location of the reaction zone. They also suggested that there existed a correlation between the chemiluminescence emission and the local rate of heat release. In studying unstable combustion, chemiluminescence emission has been extensively used to characterize temporal fluctuation in both the overall heat release and the spatial distribution of the local heat release (Langhorne, 1988; Lee et al., 2000; Paschereit and Gutmark, 2002).

Two dimensional chemiluminescence emission images obtained by ICCD camera were used in present study to see the flame structure which represented the spatial distributions of heat release during unstable combustion. It must be remembered that emission spectroscopy techniques are line-of-sight one. Since it did not reveal the cross-sectional structure of the flame, some deconvolution procedures including Abel transformation and onion-peeling have often been used to reconstruct the 2D flame structure. Although the uncertainty associated with the axisymmetric assumptions existed, the insights gained from these tomographic analyses usually outweigh those errors. In this study, simultaneous measurements of heat release and pressure were made to obtain the Rayleigh index distribution which showed the system damping and gain characteristics.

There is no doubt that the use of a non-intrusive, laser-based method for temperature determination is superior to the probe techniques, in particular, in the highly unsteady flames such as unstable combustion. CARS thermometry is one among the well established non-intrusive diagnostic tools that allows temporally and spatially resolved temperature measurements. It has been applied to numerous laboratory-scale and practical combustion systems and the fundamentals on CARS technique has been described in some articles (Eckbreth, 1988; Stricker and Meier, 1993). It could be found that temperature measurement using CARS and comparisons with model predictions were made in several works (Bradley et al., 1998). More recently, CARS tem-

perature measurements were made with other laser techniques such as laser Doppler velocimetry (LDV) or planar laser induced fluorescence (PLIF) by several researcher groups (Hedman et al., 2002 ; Foglesong et al., 1999 ; Woodmansee, 2001 ; Foglesong, 2001). However, although many experimental studies have been done in a lean premixed combustor, there was little article on the measurements of phase-resolved gas temperature under unstable combustion condition. Most of measurements were restricted to velocity, pressure fluctuations and visualization of flame structure by using CH^*, OH^*, CO_2^* or PLIF techniques. In these regards, the present paper aims to provide information necessary for further understanding of combustion-acoustic interaction in an unstable combustor. Another motivation for temperature measurement is that most of chemical reactions in a flame, which are responsible for the heat release or the formation of pollutants, are highly dependent on temperature. Therefore, the local heat release rate obtained from OH emission spectroscopy and the determination of temperature from CARS technique would be expected to play an important role in better understanding of thermo-acoustic mechanisms.

2. Experimental Details

2.1 Combustor

Figure 1 showed a schematic of optically accessible and laboratory-scale dump combustor which was a duplicate of that employed by Santavicca and co-workers (Shih et al., 1996 ; Jones et al., 1999). The combustor consists of mixing section (13.7 mm i.d., 760 mm long) where fuel is mixed with air and combustion section (42 mm i.d., 380 mm long). In studying flame structure using OH emission spectroscopy, quartz tube was used as combustion section. However, for CARS measurements, it was replaced with stainless-steel one since the diameter of quartz tube was so small that the focusing point of the laser beams damaged the tube surface. To circumvent this problem, as shown in Fig. 1, window arrangement has been located remote from the laser beam focal

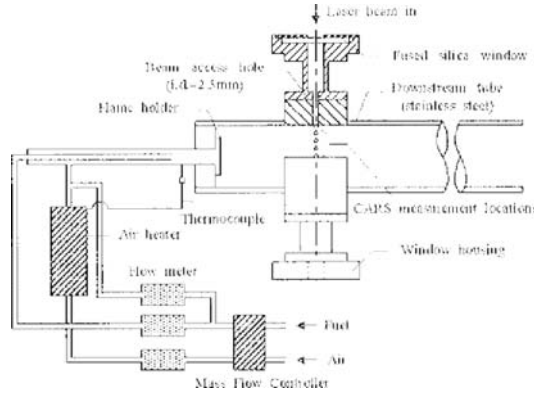

Fig. 1 Schematic diagram of the dump combustor and optical scheme for CARS temperature measurements

point. This optical scheme of CARS measurement has been adapted from other article (Bradley et. al., 1998). Air was delivered to a mixing section through the mass flow controller under atmosphere pressure, then it was heated to a temperature about 650K using the temperature controlled 2 kW air heater to simulate actual temperature at the gas turbine compressor exit.

2.2 OH chemiluminescence emission measurements

ICCD camera was used to record the OH chemiluminescence images of unstable flames. Measurements were phase-synchronized with the pressure signal obtained from sound level meter, which location and orientation were kept constant to ensure the consistency of measurements. Sequences of images which show the temporal and spatial evolution of the heat release distribution during one period of the pressure oscillation were obtained. A tomographic deconvolution procedure, as described in introduction section, was used to extract the two-dimensional heat release distribution from the original line-of-sight images. The three point Abel inversion has been used in present study based on ease of calculation and relative noise performances. Excellent review on tomographic deconvolution including the method used in this study was provided elsewhere (Dasch, 1992). The exposure time of the ICCD camera was set as 1 μs and 50

individual images were averaged to represent the heat release structure at each phase. 10 nm bandwidth filter centered at the wavelength of 310 nm was used. Equivalence ratios were in the range from 0.5 to 0.89 in this study.

2.3 CARS temperature measurements

A frequency-doubled Nd : YAG laser (Continuum, Surelite II) which produced light of 532 nm having about 200 mJ pulse energy and 7~8 ns pulse duration was used. Repetition rate was determined by the dominant frequency of fluctuating pressure signal to measure the temperature as a function of pressure phase. Details on optical arrangement of broadband mobile CARS system could be found in previously published article (Hahn et al., 1997), where the uncertainty of the averaged CARS temperature in present work has been reported to be estimated <2% in the temperature range from 1000 to 2400K. CARS measurements volume could be assumed as a cylinder which had 100 μm diameter and 1~2 mm long.

The schematic of CARS temperature measurement system was shown in Fig. 2(a). A microphone-based sound level meter (SLM) was used to sense the acoustic pressure signals. Since the output signal was too weak to use it as a laser trigger signal, it was sent to control circuit system which was composed of amplifier and counter. The purpose of counter circuit was producing a wave signal which has frequency of about 10 Hz, since the laser head lamps must flash at approximately the same frequency that the system was optimized. The output voltage has been amplified up to 5V by amplifier circuit. To provide TTL negative going signal (5V → 0V) for the laser operation, output signal coming through the circuit system was sent to delay generator (DG-535). The signal synchronization chart employed in present study was schematically shown in Fig. 2(b). We could set a typical phase of pressure cycle by changing α, because β which meant the time delay between flash lamp and Q-switched was fixed as 150 μs for CARS temperature measurements. Temperature data obtained at two axial locations which displayed different Rayleigh index characteristics at overall equivalence ratio near the blowout limit were presented. At every measurement conditions, a total of 500 single-shot spectra were acquired and approximately 0~10% of the spectra which displayed the lower temperature than the inlet air temperature were discarded. And 100 single-shot background spectra were also obtained to account for the varia

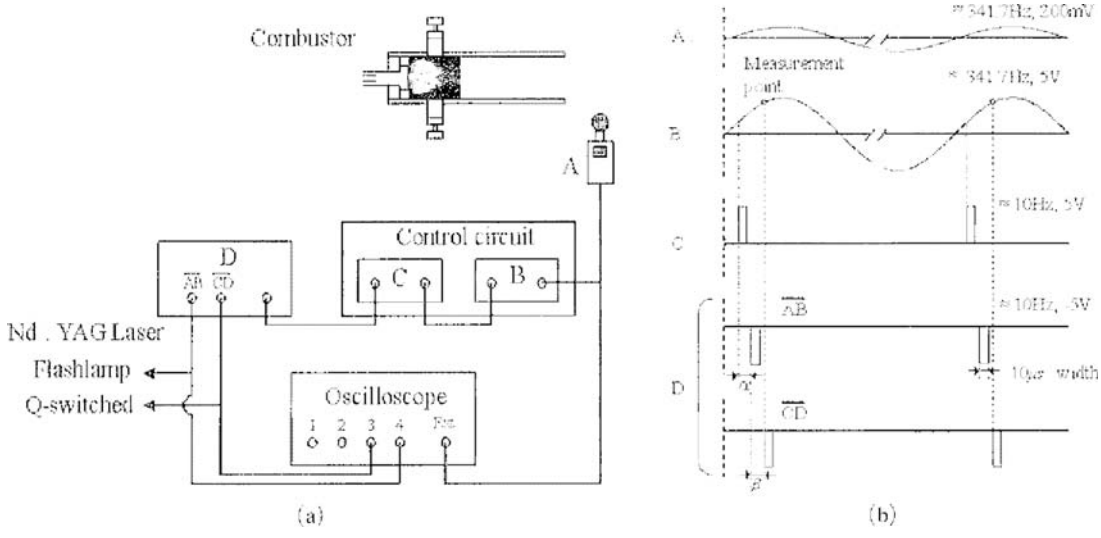

Fig. 2 (a) Schematic diagram of experimental apparatus and (b) Chart for signal synchronization ; A, sound level meter (SLM) ; B, amplifier circuit ; C, counter circuit ; D, delay generator (DG-535) ; α, time delay between external trigger and flash-lamp signal, β, time delay between flash-lamp and Q-switched signal

tions in the background signal at a particular location.

3. Results and Discussions

A typical pressure trace during unstable combustion was shown in Fig. 3(a), along with the corresponding dominant frequency in Fig. 3(b). Generally, for proper interpretation of pressure, it often required some knowledge on the mode of the instability. Though the mode could be determined by measuring pressures at several locations in the combustor, in case of the acoustic frequencies of the different modes were well separated like the case shown in Fig. 3(b), it could be estimated by following simple equation ;

$$f(Hz) = \frac{a}{l} \cdot \frac{1}{n} \quad (\text{where, } a = \sqrt{kRT}) \qquad (1)$$

where f is the frequency, a is the sound velocity, l is the length of combustor, n is the value of mode, k is the specific heat ratio, R is gas constant and T is the temperature in the combustor. Assuming the temperature in the combustor as 1100K, the calculated frequency represents value of 364 Hz. Comparing this to the measured dominant frequency of 341.7 Hz, the mode of the instability was found to be longitudinal, quarter wave one. In present study, the dominant frequency was determined not to analyze the pressure data itself but to use it as a trigger source in measuring OH chemiluminescence emission images and gas temperatures. Hence, though the pressure signal obtained at the exit of the combustor by using sound level meter could be different from that at flames in amplitude and phase in some degree, the measurement of OH chemiluminescence and temperature could be expected to be phase-synchronized reasonably.

Phase-resolved OH chemiluminescence images representing the evolution of flame structure during one period of unstable combustion were acquired at the equivalence ratio of 0.63 and shown in Fig. 4. The left half of each picture is line-of-sight integrated image and the right half is corresponding Abel transformed one. From visual inspection, it could be observed that flame anchored on the centerbody gradually extended

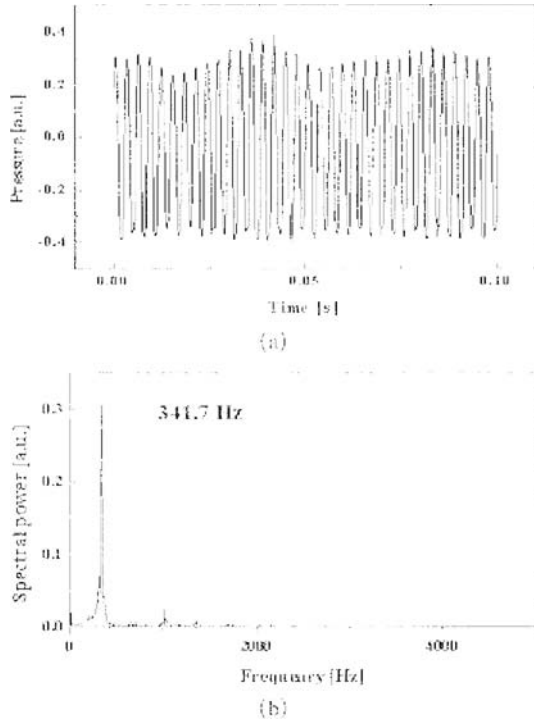

Fig. 3 (a) A typical pressure trace with respect to time and (b) its corresponding frequency spectrum showing dominant frequency of 341.7 Hz

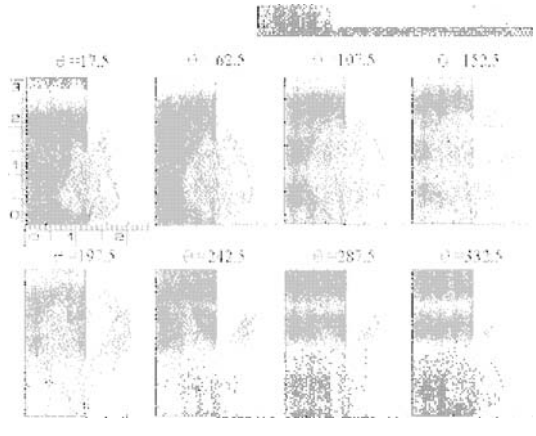

Fig. 4 Phase-resolved flame structure images during one period of unstable combustion at the equivalence ratio of 0.63 (the left half of each picture is line-of-sight image and the right half is corresponding Abel transformed one)

outward into the recirculation zone, in particular, the variations of the flame structure were very nearly in phase with the pressure oscillation. It suggested that flame structure played a role in the observed heat release fluctuations. Similar observations based on flame length and/or area fluctuations could be found elsewhere (Reuter et al., 1990; Venkataraman et al., 1999). In addition, a large change has been found in the overall intensity of OH chemiluminescence indicating the heat release of a whole flame. From a standpoint of using the intensity of chemiluminescence emission as an indicator of the heat release, the functional relationship between these two quantities were investigated in the following figure in detail.

To check the dependency of OH chemiluminescence intensity, the global heat release rates with respect to the equivalence ratio ranged from near blowout limit to near stoichiometric condition were shown in Fig. 5(a). It was notable that the intensity of OH chemiluminescence at each phase angle varied in a nearly sinusoidal manner and images indicating maximum and minimum heat releases also occurred at the corresponding phases of pressure as stated previously. These results also showed a good agreement with Rayleigh's criterion which stated that the fluctuating heat release had to be in phase with the fluctuating pressure for unstable combustion. Moreover, its amplitude was found to be larger at the fuel-richer condition.

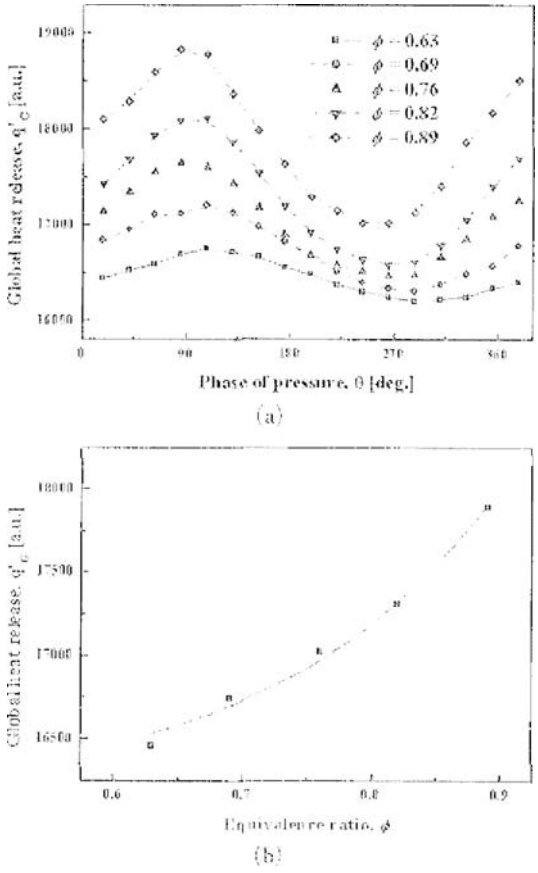

Fig. 5 Profiles of (a) global heat release with respect to the phase of pressure and (b) global heat release obtained from several different equivalence ratio conditions

To see the effect of equivalence ratio on the overall OH chemiluminescence intensity clearly, the overall chemiluminescence intensity for each equivalence ratio was provided in Fig. 5(b). It could be observed that the overall OH intensity was increased exponentially with equivalence ratio, which could be attributed to the exponential temperature dependence of the reaction rate for the formation of OH.

Two dimensional heat release images, shown in Fig. 4, were correlated with the pressure fluctuation to further explore the mutual coupling between the pressure and heat release fluctuations. The strength of the coupling could be quantified by the Rayleigh index, $R(x, y)$, which was given by following equation

$$R(x, y) = \frac{1}{\tau}\int_{\tau} p'(x, y, t)\cdot q'(x, y, t)\,dt \quad (2)$$

where, t is time, τ is the period of instability, p' is the pressure fluctuation and q' is the heat release fluctuation. Moreover, the pressure term of $p'(x, y, t)$ in Eq. 2 could be assumed as a function of time only in case that the wavelength of pressure oscillation was much longer than the length of the flame (Lee and Santavicca, 2003). This assumption was reasonably valid in present study because the flame length ($\leq$5 cm) was much shorter than the calculated wavelength of the pressure wave. Rayleigh index distributions obtained at different equivalence ratio were ($\approx$ 180 cm) provided in Fig. 6. In case of fuel lean

condition (Fig. 6(a)), regions of positive Rayleigh index which represented strong interactions between acoustic oscillations and unsteady heat release could be found immediately behind the centerbody (regions indicated as "a" and "d"). In the fuel-richer case (Fig. 6(c)), opposite trend to the former case, the instability was strongly damped at these regions of "a" and "d" while appreciable driving regions could be observed along the shear layer between the dump plane and the centerbody recirculation zone (regions of "b" and "e"). This result also showed that it could be used to identify the variations in the damping and/or driving regions of instability with respect

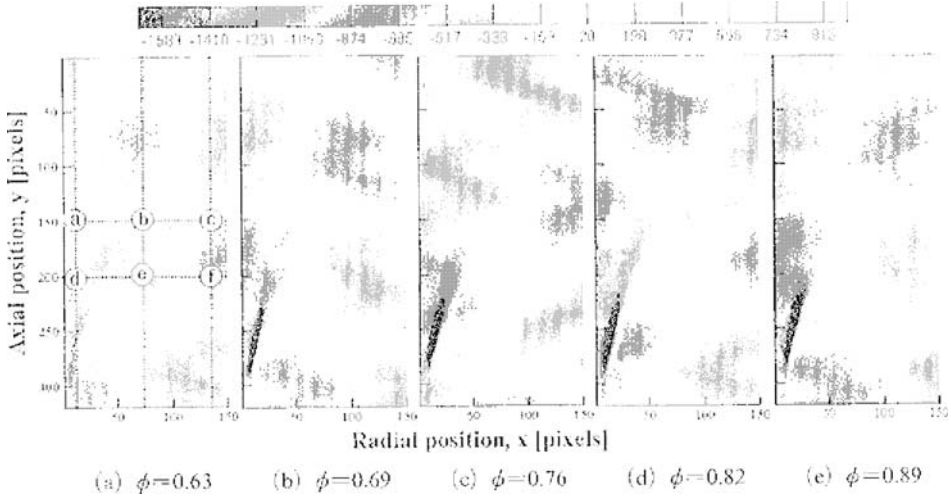

Fig. 6 Two dimensional Rayleigh index distributions obtained at different equivalence ratio conditions which showed the features of unstable combustion

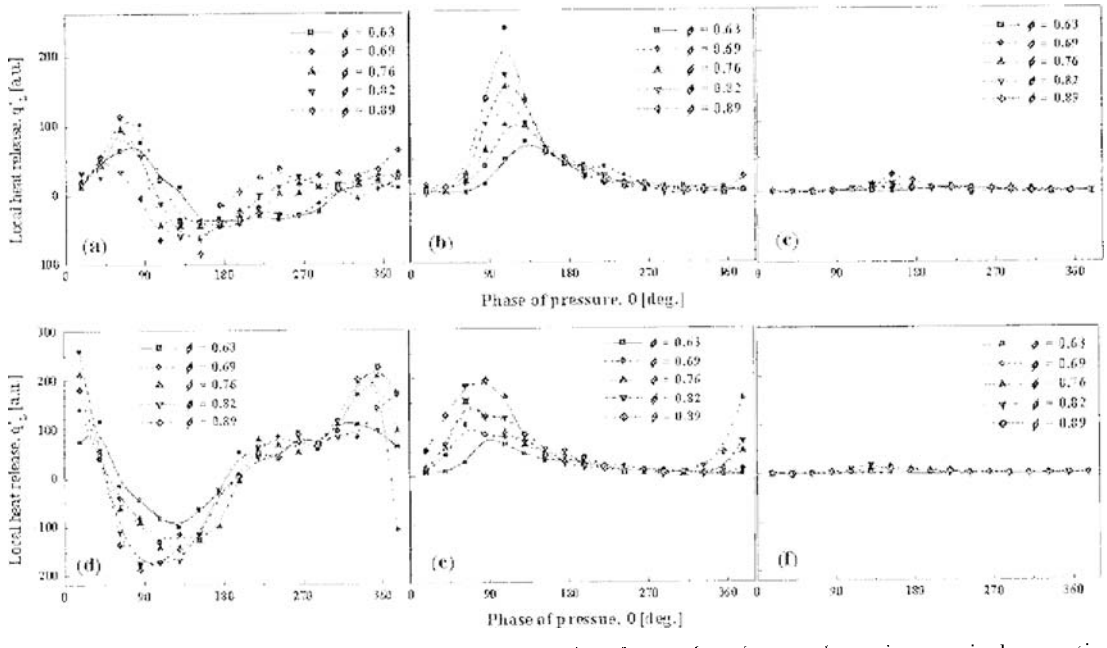

Fig. 7 Profiles of local heat release rate obtained from six reference locations at the various equivalence ratio conditions

to equivalence ratio (Moon et al., 2004).

For further investigation, local heat release rates obtained at six reference locations, as indicated in Fig. 6, were presented in Fig. 7. First, at the location of "a," it could be found that the characteristic of heat release rate at the fuel-leanest condition showed most in-phase with the pressure wave while those magnitudes were similar. And most of profiles at the location of "d" showed nearly out-of-phase ones with pressure fluctuation, which was consistent with the previous results showing the negative Rayleigh index at this location. On the other hand, at the location of "b," it also could be observed that the heat release rate became more in-phase with pressure as well as the magnitude of heat release was increased as the equivalence ratio went richer.

Temperature measurements were also made at typical condition which obtained the OH chemiluminescence images. It has been motivated by the fact that most of chemical reactions, which were responsible for the heat release, were highly dependent on temperature. Another motivation was that there have been little works which investigated periodic variations of temperature during unstable combustion. In these regards, phase-resolved single-pulse temperature measurements using CARS technique were performed to provide fundamental data for better understanding the thermo-acoustic interactions as well as correlate the measured temperature with local heat release rate. Temperature probability density functions (PDFs) were constructed from 500 single-pulse measurements at several locations of interest throughout the combustor at various experimental conditions. Fig. 8 showed the results of temperature PDFs, for instance, acquired at the location of "a" (in Fig. 6). The 12 plates have shown the temperature PDFs obtained in phase with the 12 points indicated on the periodic pressure cycle

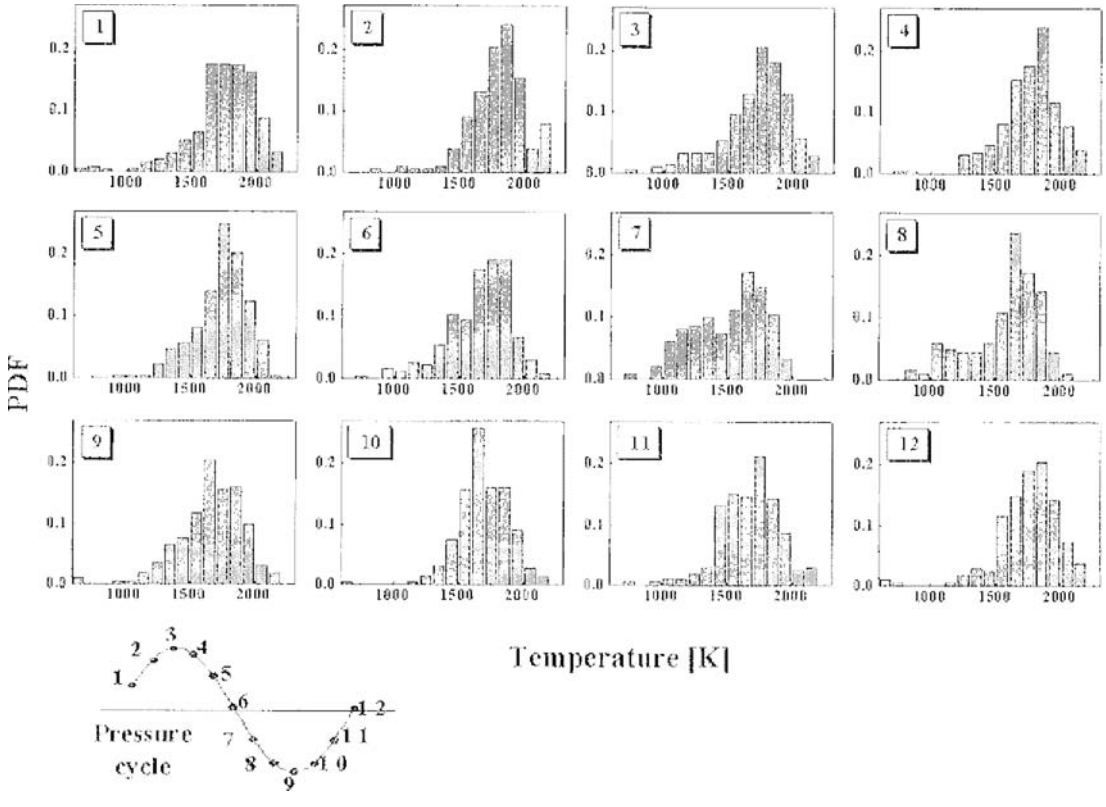

Fig. 8 Temperature PDFs obtained at the equally spaced 12 phases of periodic pressure cycle at the location of "a" (in Fig. 6) and equivalence ratio of 0.63

as shown in the lower left corner. The shape of each PDF distribution has a physical significance giving insights into the nature of the temperature fluctuations at a given location (Foglesong, 2001). For example, beta distribution implies a predominance of temperature value around the peak of the distribution with significant contributions of either higher or lower temperature, while bimodal distribution could be interpreted as the existence of two gas streams whose temperatures vary widely and are centered at either one of the contiguous peaks. Additional insights regarding the flow structure under reacting condition also could be obtained by examining the spatial variation in the shape of the temperature PDFs (Lee et al., 2004).

Among temperature histograms shown in Fig. 8, representative ones obtained at typical phases of pressure were provided in Fig. 9 to see the temperature fluctuation characteristics. Though there were little changes in the shape of histograms, it could be found that the temperature distributions have been changed during a period of the pressure wave periodically. And the temperature value with the highest probability within the histogram also changed consecutively from 1650K to 1850K, and vice versa.

For further investigation on the dynamic behavior of temperature, phase-resolved mean temperatures and corresponding normalized standard deviations acquired at the locations of "a" and "c"(in Fig. 6) were shown in Fig. 10. Remind that the Rayleigh index at the location of "a" showed positive value while that at the location of "c" was negative. The profiles of phase-resolved mean temperatures at these locations also showed similar trends with those of local heat release rates as shown in Fig. 7. From these observations, it could be assumed that there existed a relationship between the measured temperature and the heat release rate obtained from OH chemiluminescence. After the standard deviations for the measured temperatures being calculated, these values were divided by the corresponding mean temperature. These results of normalized standard deviation were also included in Fig. 10. This method was analogous to that done with fluctuating velocity data to determine a local turbulent intensity. Details on this could be found from other article (Hedman et al. 2002). The profile of normalized standard deviation at the location of "c", for example, showed nearly constant value, which also indicated the precision of CARS technique. However, it was characterized by a relatively broader temperature distribution than the case of single-shot CARS measurements in a temperature stable medium which usually had the standard deviation of 100~150K. It was probably due to the evolution of flame

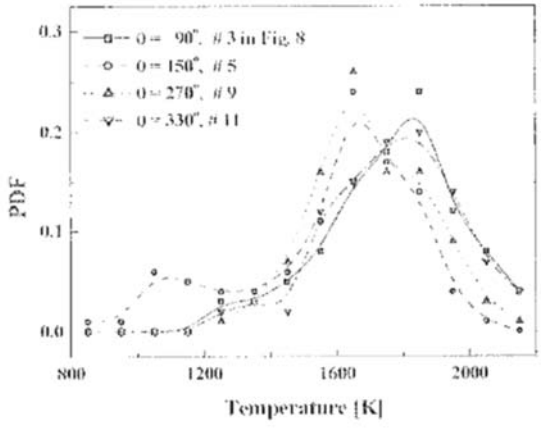

Fig. 9 Representative temperature histograms at different phases of pressure obtained at the location of "a" (in Fig. 6) and equivalence ratio of 0.63

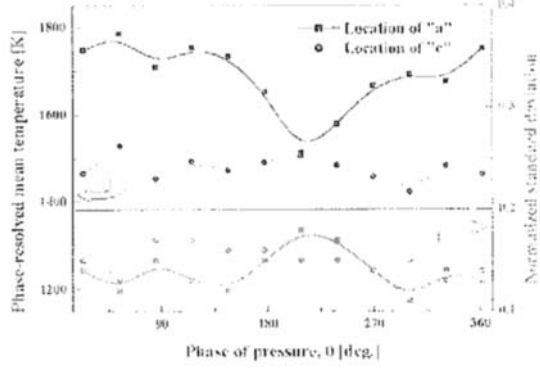

Fig. 10 Profiles of (a) phase-resolved mean temperature and (b) normalized standard deviation obtained at two locations which showed the different Rayleigh index characteristics at the equivalence ratio of 0.63

structure induced by unstable combustion. It was also notable that maximum temperature difference among those phase-resolved mean temperatures reached up to 280K. For reference, the phase-resolved mean temperature at the poor fuel/air mixed condition, not shown here, varied by almost 500K over one period. It suggested that temperature measurements during unstable combustion should be made under consideration of pressure oscillations.

The profiles of phase-resolved mean temperature and local heat release rate were shown in Fig. 11 to see the relationship. From visual inspection, it could be found that these two profiles were in phase qualitatively and the local heat release obtained from OH chemiluminescence showed low values in typical range of pressure phase, that is, when the measured temperatures displayed value lower than 1650K approximately. It probably suggested that the intensity of OH chemiluminescence was highly dependent on temperature. The profile of global heat release obtained from a whole flame, for reference, was also included in Fig. 11. It showed somewhat different characteristics compared with that of local heat release while strong coupling between pressure and heat release fluctuations was reconfirmed by the observation that the profile of pressure led the heat release fluctuation by approximately 20 deg.

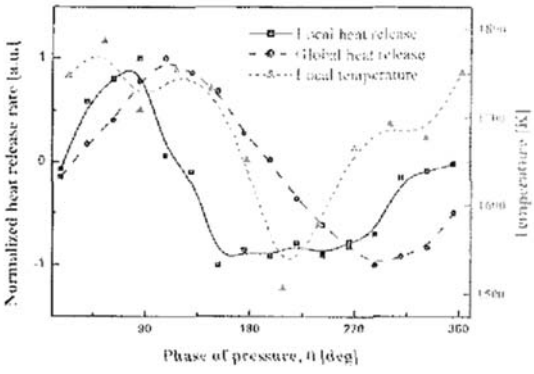

Fig. 11 Profiles of global heat release, local heat release and temperatures with respect to the phase of pressure obtained at the location of "a" (in Fig. 6) and equivalence ratio of 0.63

4. Conclusions

A study on the flame structure and phase-resolved gas temperature during unstable combustion in a lean premixed dump combustor was performed by means of OH emission and CARS spectroscopy respectively. Flame structure images showed its evolution and nearly in-phase characteristics with respect to pressure phase during one period of instability. The use of OH chemiluminescence intensity as an indicator of heat release was also investigated and its linear relationship between the two quantities could be confirmed. In combining these results with the pressure fluctuations, the coupling strength between pressure and heat release fluctuations could be quantified by the Rayleigh index, which provided an insight on the damping and/or driving regions of instability at typical equivalence ratio condition.

The present work also provided non-existent phase-resolved temperature data to add fundamental knowledge of combustion-acoustic interaction in an unstable combustor. Results showed that the shapes of temperature distributions obtained at typical location were unchanged, while the temperature with the highest probability within the histogram varied periodically from 1650K to 1850K, and vice versa. It also could be found that maximum temperature difference among these phase-resolved mean temperatures reached up to 280K. At the fuel/air poor mixing condition, though not shown here, those phase-resolved mean temperatures varied by almost 500K over one period. It meant that phase-synchronized temperature measurements should be made during unstable combustion with respect to the pressure oscillations. Lastly, qualitatively in-phase relationship between the profiles of phase-resolved mean temperature and local heat release rate was observed.

Acknowledgments

CARS temperature measurements in present work have been done in Korea Research Institute

of Standards and Science (KRISS) and we gratefully thanks to researchers in KRISS.

References

Bradley, D., Gaskell, P. H., Gu, X. J., Lawes, M. and Scott, M. J., 1998, "Premixed Turbulent Flame Instability and NO Formation in a Lean-burn Swirl Burner," *Combust. Flame*, Vol. 115, pp. 515~538.

Docquier, N. and Candel, S., 2002, "Combustion Control and Sensors: A Review," *Prog. Energy Combust. Sci.*, Vol. 28, pp. 107~150.

Dandy, D. S. and Vosen, S. R., 1992, "Numerical and Experimental Studies of Hydroxyl Radical Chemiluminescence in Methane-Air Flames," *Combust. Sci. and Tech.*, Vol. 82, pp. 131-150.

Dasch, C. J., 1992, "One-dimensional Tomography: A comparison of Abel, Onion-peeling, and Filtered Backprojection Methods," *Appl. Opt*, Vol. 31, No. 8, pp. 1146~1152.

Eckbreth, A. C., 1988, "Laser Diagnostics for Combustion Temperature and Species," Vol. 7, pp. 220~300.

Foglesong, R. E., Frazier, T. R., Flamand, L. M., Peters, J. E. and Lucht, R. P., 1999, "Flame Structure and Emissions Characteristics of a Lean Premixed Gas Turbine Combustor," *AIAA paper* 99-2399.

Foglesong, R. E., 2001, "Experimental Investigation of a Lean, Premixed Gas Turbine Combustor Using Advanced Laser Diagnostics," *Ph. D. thesis. University of Illinois at Urbana-Champaign.*

Hahn, J. W., Park, C. W. and Park, S. N., 1997, "Broadband Coherent Anti-Stokes Raman Spectroscopy with a Modeless Dye Laser," *Appl. Opt*, Vol. 36, pp. 6722~6728.

Hedman, P. O., Flores, D. V. and Fletcher, T. H., 2002, "Observations of Flame Behavior in a Laboratory-scale Pre-mixed Natural gas/Air Gas Turbine Combustor from CARS Temperature Measurements," *ASME*, GT-2002-30054.

Jones, C. M., Lee, J. G., and Santavicca, D. A., 1999, "Closed-loop Active Control of Combustion Instabilities Using Subharmonic Secondary Fuel Injection," *J. Propulsion and power*, Vol. 15, No. 4, pp. 584~590.

Lee, J. G., Kim, K. and Santavicca, D. A., 2000, "Measurement of Equivalence Ratio Fluctuation and Its Effect in Heat Release During Unstable Combustion," *Proc. Combust. Instit.*, Vol. 28, pp. 415~421.

Lee, J. G. and Santavicca D. A., 2003, "Experimental Diagnostics for the Study of Combustion Instabilities in Lean Premixed Combustors," *J. Propulsion and power*, Vol. 19, No. 5, pp. 735~750.

Lee, S. Y., Seo, S., Broda, S. P. and Santoro, R. J., 2000, "An Experimental Estimation of Mean Reaction Rate and Flame Structure During Combustion Instability in a Lean Premixed Gas Turbine Combustor," *Proc. Combust. Instit.*, Vol. 28, pp. 775~782.

Lefevbre, A. H., 1999, "Gas Turbine Combustion," *2nd Ed., Taylor & Francis*, pp. 324~344.

Langhorne, P. J., 1988, "Reheat Buzz: An Acoustically Coupled Combustion Instability. Part 1. Experiment," *Journal of Fluid Mechanics*, Vol. 193, pp. 417~443.

Lee, J. H., Jeon, C. H., Hahn, J. W., Park, C. W., Han, Y. M., Yang, S. S., Lee, D. S. and Chang, Y. J., 2004, "CARS Temperature Measurement in a Liquid Kerosene fueled Gas Turbine Combustor Sector Rigs," *6th COMODIA*, pp. 13~19.

McDonell, V. G., and Samuelsen, G. S., 2000, "Measurement of Fuel Mixing and Transport Processes in Gas Turbine Combustion," *Meas. Sci. Technol.*, Vol. 11, pp. 870~886.

McManus, K. R., Poinsot, T. and Candel, S. M., 1993, "A Review of Active Control of Combustion Instabilities," *Prog. Energy Combust. Sci.*, Vol. 19, pp. 1~29.

Moon, G. F., Lee, J. H., Jeon, C. H. and Chang, Y. J., 2004, "Experimental Study on Heat Release in a Lean Premixed Dump Combustor Using OH Chemiluminescence Images," *Trans. of the KSME (B)*, Vol. 28, No. 11, pp. 1368~1375.

Najm, H. N., Paul, P. H., Mueller, C. J. and Wyckoff, P. S., 1998, "On the Adequacy of Certain Experimental Observables as Measurements of Flame Burning Rate," *Combustion and*

Flame, Vol. 113, pp. 312~332.

Paschereit, C. O. and Gutmark, E. J., 2002, "Enhanced Performance of a Gas-Turbine Combustor Using Miniature Vortex Generators," *Proc. Combust. Instit.*, Vol. 29, pp. 123~129.

Reuter, D. M., Hegde, U. G., and Zinn, B. T., 1990, "Flowfield Measurements in an Unstable Ramjet Burner," *J. Propulsion and power*, Vol. 6, No. 6, pp. 680~685.

Samaniego, J. M., Egolfopoulos, F. N. and Bowman, C. T., 1995, "CO_2* Chemiluminescence in Premixed Flames," *Combust. Sci. and Tech.*, Vol. 109, pp. 312~332.

Shih, W. P., Lee, J. and Santavicca, D. A., 1996, "Stability and Emissions Characteristics of a Lean Premixed Gas Turbine Combustor," *Proc. Combust. Instit.*, Vol. 26, pp. 2771~2778.

Seo, S., 2003, "Combustion Instability Mechanism of a Lean Premixed Gas Turbine Combustor," *KSME International Journal*, Vol. 17, No. 6, pp. 906~913.

Stricker, W. and Meier, W., 1993, "The Use of CARS for Temperature Measurements in Practical Flames," *Trends in Appl. Spectroscopy*, Vol. 1, pp. 231~260.

Venkataraman, K. K., Preston, L. H., Simons, D. W., Lee, B. J., Lee, J. G. and Santavicca, D. A., 1999, "Mechanism of Combustion Instability in Lean Premixed Dump Combustor," *J. Propulsion and power*, Vol. 15, pp. 909~918.

Woodmansee, M. A., 2001, "Experimental Measurements of Pressure, Temperature, and Density Using High Resolution N_2 Coherent Anti-stokes Raman Scattering," *Ph. D. thesis. University of Illinois at Urbana-Champaign.*

Zinn, B. T. and Neumeier, Y., 1997, "An overview of Active Control of Combustion Instabilities," *AIAA paper* 97-0461.